Spectral sharpening of the Pt L edges by high-resolution x-ray emission

F. M. F. de Groot,[1] M. H. Krisch,[2] and J. Vogel[3]

[1]*Department of Inorganic Chemistry and Catalysis, Utrecht University, Sorbonnelaan 16, 3584 CA, Utrecht, The Netherlands*
[2]*ESRF, BP 220, F-38043 Grenoble, France*
[3]*Laboratoire Louis Néel (CNRS), 25, Avenue des Martyrs, BP 166, 38042 Grenoble, France*

The platinum $2p_{3/2}$, $2p_{1/2}$, and $2s$ x-ray absorption spectra, recorded by monitoring the fluorescence intensity with eV energy resolution, show a spectral broadening that is significantly less than the $2p$ and $2s$ core hole lifetime broadening. The background of such spectral sharpening is discussed. It is shown, experimentally as well as theoretically, that the lifetime broadening of the $2p$ and $2s$ core holes is replaced by a new lifetime broadening. It is demonstrated that from the combination of normal x-ray absorption, selective x-ray absorption, and x-ray emission, the individual lifetimes of all participating core states can be determined. The difference between the $5d_{5/2}$ and $5d_{3/2}$ densities of states can be obtained from a combination of the $2p_{1/2}$ and $2p_{3/2}$ x-ray absorption spectra. The present spectra are limited by the experimental resolution. With the prospect of an improved experimental resolution for x-ray excitation and decay, the Pt edge absorption spectra could be obtained with even better resolution, thus providing a high-resolution hard x-ray probe of the empty density of states with important advantages for in-situ and high-pressure studies.

I. INTRODUCTION

X-ray absorption spectroscopy is a widely spread technique to study the electronic properties of materials. The absorption edge position can be correlated with the valence of the system, and in many cases the x-ray absorption spectrum (XAS) yields a signal that is proportional to the empty density of states (DOS).[1] Due to the local character of x-ray absorption and the optical dipole selection rule, $1s$ (K edge) x-ray absorption probes the element specific p-projected DOS, while $2p$ ($L_{2,3}$) x-ray absorption probes the s- and d-projected DOS, etc. The close correspondence between XAS and DOS is, however, destroyed if the core and valence wave functions overlap strongly, as for example in the case of the $3d$ metal L edges.[2–4] Common to all x-ray absorption spectra is their intrinsic energy broadening, arising from the finite lifetime of the deep core hole, created by the absorption process. This broadening is strongly dependent on the atomic number Z and the atomic shell involved in the absorption process. Attempts to overcome this fundamental limitation have been first undertaken by Hämäläinen and co-workers.[5] They recorded the Dy L_3 near-edge spectrum, monitoring the Dy $L\alpha_1$ fluorescence with an energy resolution better than the core hole lifetime broadening, and indeed observed a much more structured spectral shape with respect to the conventional XAS spectrum. A similar approach, using nonradiative decay channels, has been developed by the groups of Sham[6–8] and Drube.[9–11] Another approach used a deconvolution of very-high-quality XAS data.[12] The two methods however, did, not yield the same spectral shape. This was attributed to the fact that in the specific case of the rare-earths, a simple one-electron picture breaks down, and many-body correlations between the $4f$ electrons and the other participating electron shells have to be taken into account.[13]

In this article we demonstrate, using platinum metal as an example, the potential of sub-lifetime resolved x-ray absorp-

tion spectroscopy. The $2p$ edges of Pt have been measured by Qi and co-workers.[14] The $2p$ XAS spectra of Pt are dominated by respectively the $2p_{1/2}$ to $5d_{3/2}$ and $2p_{3/2}$ to $5d_{5/2}$ dipole transitions. It has been shown that the intensity of the leading edge, i.e., the white line, reflects the number of holes in the $5d$ band.[14,15] While the $2p_{3/2}$ edge shows a distinct white line, the $2p_{1/2}$ edge only shows a small structure. This effect is ascribed to the fact that the $2p_{1/2}$ edge only makes transitions to the $5d_{3/2}$ band that is filled in case of Pt metal. We recorded the $2s$, $2p_{1/2}$, and $2p_{3/2}$ x-ray absorption edges, monitoring the $2s5p$, $2p_{1/2}4d$, and $2p_{3/2}3d_{5/2}$ x-ray emission channels, respectively, with a spectrometer energy resolution of typically 2 eV. The spectra display a significant sharpening with respect to the conventional XAS spectra, and reveal a white-line feature as well for the $2p_{1/2}$ absorption edge. We furthermore show that from the combination of normal x-ray absorption, selective x-ray absorption, and x-ray emission, the individual lifetime broadening of all participating core states can be determined.

II. EXPERIMENT

The experiment was performed on the beamline ID26 at the European Synchrotron Radiation Facility (ESRF). The incident linearly polarized x rays produced by a linear 42 mm undulator were monochromatized by a cryogenically cooled silicon (111) double crystal monochromator, providing an energy bandwidth of approximately 2.0 eV. The beam impinging on the sample was sized down to 0.6 mm horizontally by 2 mm vertically. These settings resulted in an incident photon flux of 3×10^{12} photons/s. The scattered radiation was analyzed in the horizontal plane by a 1 m Rowland circle spectrometer, utilizing the (931) and (880) reflection order from a spherically bent silicon crystal. The inelastic x-ray (IXS) spectra were recorded at a scattering angle of 90 degrees, and the solid angle spanned by the analyzer crystal was 3000 mrad^2. The refocused scattered x rays from the

crystal analyzer were detected by a Peltier cooled silicon diode in photon counting mode. The overall experimental resolution was 2.3 eV. The $h_2 + k_2 + l_2$ value of Si(931) is 91, implying that the detection energy (in eV) is given as 10 889/sin φ, where φ is the angle of analyzer crystal. The Si(931) crystal was used for the Pt valence band emission and the $4d \rightarrow 2p_{3/2}$ emission. Si(880) has a $h_2 + k_2 + l_2$ value of 128 that yields energies according to 12 915/sin φ. It was used for the $2s5p$ emission and the $2p_{1/2}3d$ emission.

The platinum sample, a high-purity foil purchased from Goodfellow, was mounted inside a vacuum chamber in order to reduce contributions from air scattering. The fluorescence spectra were recorded at a fixed incident photon energy, well above the respective x-ray absorption edge energies, and scanning the energy of the spectrometer. The selective x-ray absorption spectra were recorded by fixing the x-ray emission energy to a value corresponding to the maximum of the fluorescence line, and varying the incident photon energy through the absorption edge. A silicon detector simultaneously recorded the total fluorescence.

III. THEORY

A. Sub-lifetime resolved x-ray absorption

By tuning the incident photon energy close to the $2p$ absorption edge, the x-ray absorption and x-ray emission processes occur coherently and the overall $2p3d$ process is described by the Kramers-Heisenberg formula:

$$I(\omega, \omega') \sim \left| \sum_{\underline{2p}} \frac{\langle 3d | \hat{e}' \cdot r | \underline{2p} \rangle \langle \underline{2p} | \hat{e} \cdot r | Pt \rangle}{E_{\underline{2p}} - E_{Pt} - \hbar\omega - i\Gamma_{2p}} \right|^2 \cdot L_{\underline{3d}} \cdot G_\omega \cdot G_{\omega'}. \tag{1}$$

This formula forms the basis of all resonant x-ray processes. The intensity (I) is given as a function of the excitation (ω) and the emission (ω') energies. The Pt ground state is excited to an intermediate state, characterized by a $2p$ core hole via the dipole operator ($\hat{e} \cdot r$). The second dipole operator ($\hat{e}' \cdot r$) describes the x-ray emission decay to the final state with a $3d$ core hole. The denominator contains the binding energy of the $2p$ core hole and its lifetime broadening. The convolution with the $3d$ final state lifetime broadening is indicated with $L_{\underline{3p}}$, whereas G_ω ($G_{\omega'}$) indicates the convolution with the experimental broadening due to monochromator (spectrometer). A resonance occurs if the excitation energy is equal to the Pt $2p$ edge. The general spectral landscape can be viewed as a two-dimensional space with axis ω and ω'. Figure 1 shows a contour-plot of the $2p_{3/2}3d$ resonant x-ray emission spectrum of Pt. The gray area is the peak maximum, which is set at 100%. The first contour-line is set at 64% and each following line represents respectively 32%, 16%, 8%, etc., as indicated in the figure. The horizontal axis shows the x-ray excitation energy. The $2p$ x-ray absorption spectrum of Pt is assumed to consist of a single resonance with an energy of approximately 11 560 eV. The vertical axis shows the final state energies with a maximum of the $2p3d$ decay at 2123 eV.

Instead of normal x-ray absorption, one can measure the x-ray absorption spectrum at a fixed emission energy. This
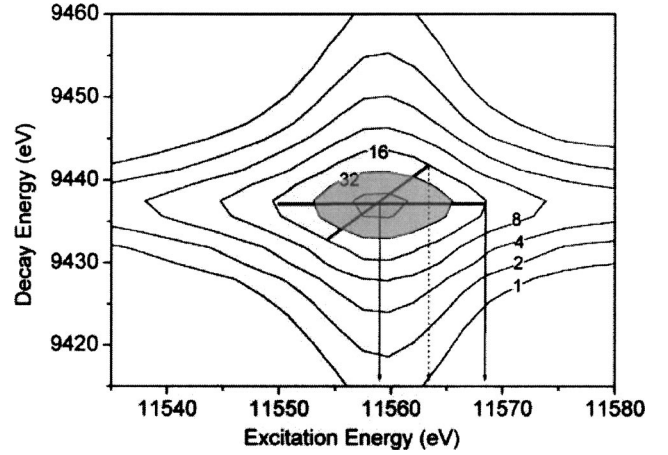

FIG. 1. Contour-plot of the $2p_{3/2}3d_{5/2}$ resonant x-ray emission spectrum of Pt. The horizontal line indicates the 16% contour of the normal x-ray absorption experiment. The diagonal line indicates the same 16% contour of the selective x-ray absorption experiment, where the arrows indicate the projection to the x-ray absorption axis.

relates to the diagonal line in Fig. 1. The effective lifetime related broadening can be easily derived from the figure, and is given by

$$\Gamma_{SEL} = 1/\sqrt{(1/\Gamma_{2p}^2) + (1/\Gamma_{3d}^2)}. \tag{2}$$

The $2p$ intermediate state lifetime broadening has been made artificially large and the half-width at the 16% contour is approximately 9.0 eV, as indicated by the two solid arrows. The broadening obtained by selective x-ray absorption measured along the diagonal is indicated by the dashed arrow and the half-width at the 16% contour is approximately 5.0 eV. For reasons of clarity we use the 16% contour to indicate the difference between x-ray absorption and selective x-ray absorption. The Lorentzian broadening thus decreases in comparing normal x-ray absorption and selective x-ray absorption. Note that this sharpening effect makes use of a projection on the horizontal axis of a cross-section through a single resonance at 45 degrees in Fig. 1. In other words, $I_{XAS}^{\omega'}(\omega)$, the absorption cross section, is detected at a fixed emission energy. One can make some objections to this approach, as this projection appears to be a kind of cheating. In the case of a single resonance there is, however, no serious problem. In the case of a series of resonances with, in particular, a series of different final state energies, the situation becomes more complex. In this case, a scan at fixed emission energy cuts through these various resonances in a rather undefined manner. For example, if one chooses a specific emission energy as the detection energy, the other resonances are intercepted away from their maximum and the obtained spectral shape of selective x-ray absorption will have a complex denotation. If one excites into the continuum, detection at fixed emission energy implies detection of the "normal fluorescence" at a fixed position. In this case the lifetime broadening is determined solely by the final state lifetime Γ_{3d}. From this discussion one can conclude that selective x-ray absorption only leads to a straightforward result in

TABLE I. The relative intensities of the four $2p5d$ transitions separated into their different j-subshells. The result derived from band structure is compared with the results from multiplet calculations. The bottom line gives the atomic multiplet results for the $2p4f$ quadrupole transitions.

$2p_{3/2}5d_{5/2}$	$2p_{3/2}5d_{3/2}$	$2p_{1/2}5d_{5/2}$	$2p_{1/2}5d_{3/2}$	Branching ratio	
8.57	1.43	**0.00**	5.00	<u>0.57</u>	Band
9.00	1.00	**0.00**	5.00	0.60	Atomic
8.95	1.05	**0.05**	4.95	0.60	10Dq=1
8.60	1.40	**0.40**	4.60	0.60	10Dq=3
8.15	1.85	**0.84**	4.16	0.60	10Dq=5
$2p_{3/2}4f_{7/2}$	$2p_{3/2}4f_{5/2}$	$2p_{1/2}4f_{7/2}$	$2p_{1/2}4f_{5/2}$		
8.57	1.43	**0.00**	5.00	0.57	Atomic
(6)	(1)		(7/2)		

those systems where all excitations are into the continuum, or to systems with a single resonance accompanied with continuum excitations. The $2p$ edge of platinum is expected to be a good example of such systems, because there is only a single resonance, associated with the holes in the $5d$-band, accompanied by excitations into the s and d continuum.

In the case of the Pt $2p$ intermediate states, there is only one resonance implying that one can decouple the excitation and the decay process and rewrite Eq. (1) for selective x-ray absorption to

$$I^{\omega'}_{\text{XAS}}(\omega)=C_{\omega'}\cdot C_{\omega}\cdot \rho(\omega)\cdot L_{\text{SEL}}\cdot G_{\omega}\cdot G_{\omega'}. \qquad (3)$$

C_{ω} and $C_{\omega'}$ are the proportionality factors of the x-ray absorption and x-ray emission cross sections and G_{ω} and $G_{\omega'}$ are the convolutions with the experimental broadening of the incident x rays (ω) and scattered x rays (ω'). $\rho(\omega)$ is the density of states and L_{SEL} is the convolution with the Lorentzian broadening using Γ_{SEL}. Equation (3) shows that, under the approximations that apply for platinum metal, selective x-ray absorption measures the same spectral shape as normal x-ray absorption, that is the, projected, density of states. The broadening by Γ_{1s} and G_{ω} is replaced by Γ_{SEL}, G_{ω}, and $G_{\omega'}$, which in the case of high-resolution excitation and detection is able to yield sharper x-ray absorption spectra than obtained normally.

B. Real space multiple scattering calculations

The simulation of the x-ray absorption spectra has been performed with the real space Green's function code FEFF8.[16] In this method the x-ray absorption coefficient is calculated from the one-electron density matrix according to the Fermi golden rule.[1] The FEFF8 code includes the final-state broadening due to core hole lifetime. We used the FEFF8 code[1] for a cluster of 55 Pt atoms that cover all Pt atoms within a 0.54 nm radius. The Pt density-of-states is calculated for the central Pt atom with respectively a $2s$, $2p_{1/2}$, and $2p_{3/2}$ core hole. A Hedin-Lundqvist potential has been used and the XANES has been calculated with a negative V_i in order to adapt the core hole lifetime broadening to the situation of selective x-ray absorption.

C. The $5d$ spin-orbit coupling

The $5d$ spin-orbit coupling splits the $5d$ valence band into two subbands. These two subbands have often been related to respectively the $2p_{1/2}$ and $2p_{3/2}$ core levels. The core hole spin-orbit splitting is approximately 1800 eV and this large value assures a pure $2p_{1/2}$, respectively $2p_{3/2}$, core state, for both edges. The $5d$ spin-orbit coupling is smaller, being approximately 2.0 eV. Most papers that analyze the $2p$ edges of the $5d$ elements assume that the $2p_{1/2}5d_{3/2}$, $2p_{3/2}5d_{5/2}$, and $2p_{3/2}5d_{3/2}$ transitions are possible. Following band structure results on Pt, a fixed ratio is assumed for these three transitions. The ratio between the $2p_{3/2}5d_{5/2}$ and $2p_{3/2}5d_{3/2}$ transitions is assumed to be 6:1, yielding overall transitions strengths as indicated in Table I.

The band structure results are confronted with multiplet calculations.[17] The atomic multiplet calculation gives the result of the relative intensities of respectively 9, 1, 0, and 5 (cf. Table I). This immediately yields the $2p_{3/2}$ to $2p_{1/2}$ ratio of 10 to 5, in accord with the $2J+1$ degeneracy of the states. In addition it yields the $5d_{5/2}$ to $5d_{3/2}$ ratio of 9 to 6, again in agreement with the $2J+1$ degeneracy of the $5d$ states. Both these ratios must be fulfilled independent of the local symmetry of the states. Note that the band structure derived results yields a branching ratio $2p_{3/2}/(2p_{3/2}+2p_{1/2})$ of 0.57 instead of the correct value of 0.60. Interestingly the value of 0.57 is exactly the atomic value for a $2p$ to $4d$ quadrupole transition (cf. Table I), though this is probably an accidental result. The atomic multiplet calculations have been modified to add a cubic crystal field. A cubic crystal field value of 3.0 eV yields approximately the same ratio for the $2p_{3/2}5d_{5/2}$ to $2p_{3/2}5d_{3/2}$ compared to the band structure result. The difference between the multiplet calculation and the band structure derived result is that the $2p_{1/2}5d_{5/2}$ transition is not forbidden in nonatomic symmetries. In contrast with what is usually assumed,[6] this implies that even in the case of a completely filled $5d_{3/2}$ band, there will be a nonzero white line intensity related to the $2p_{1/2}5d_{5/2}$ transition at the L_2 edge.

IV. RESULTS AND DISCUSSION

A. The x-ray emission spectra

To measure the $2s$, $2p_{1/2}$, and $2p_{3/2}$ x-ray absorption spectra with sub-lifetime resolution, an x-ray emission chan-

TABLE II. The energies and lifetime broadenings for the core levels and transitions used in the x-ray absorption and x-ray emission experiments. The XPS column gives the values tabulated in Ref. 20. XAS gives the experimentally determined broadenings from XAS and selective XAS. The XES column gives the, corrected, x-ray emission values.

| | | Lifetime broadenings | | |
	Energy	XPS	XAS	XES
$2p_{1/2}$	13 273	5.9	6.5	⋯
$3d_{3/2}$	2202	3.0	1.7	⋯
$2p_{1/2}3d_{3/2}$	11 071	8.9	8.2	7.9
$2p_{3/2}$	11 564	5.3	6.7	⋯
$4d_{5/2}$	315	3.6	1.9	⋯
$2p_{3/2}4d_{5/2}$	11 250	8.9	8.6	9.0
$2s$	13 880	9.4	⋯	⋯
$3p$	2645	9.0	⋯	⋯
$2s3p$	11 225	18.4	⋯	18

nel must be chosen for each edge. Criteria for the used x-ray emission channel are (*i*) the intensity, (*ii*) the energy, and (*iii*) its lifetime broadening. It is clear that one searches for maximum emission intensity and a narrow lifetime broadening. Concerning the experiment, the most critical parameter is the x-ray emission energy because that determines the choice of backscattering crystal and its resolution.

The strongest x-ray emission channels are the p to d and s to p channels. The availability and resolution criteria of the backscattering crystal determine the choice for respectively the $2s3p$, $2p_{1/2}3d_{3/2}$, and $2p_{3/2}4d$ x-ray emission spectra. Their binding energies and approximate transition energies are indicated in Table II. The $2p_{3/2}4d$ emission and the $2s3p$ emission have the same energy and hence overlap if one excites above the $2s$ edge at 13 880 eV. Figure 2 shows the x-ray emission energy range between 11 220 and 11 280 eV at excitation energies of respectively 11 568 eV and 11 610
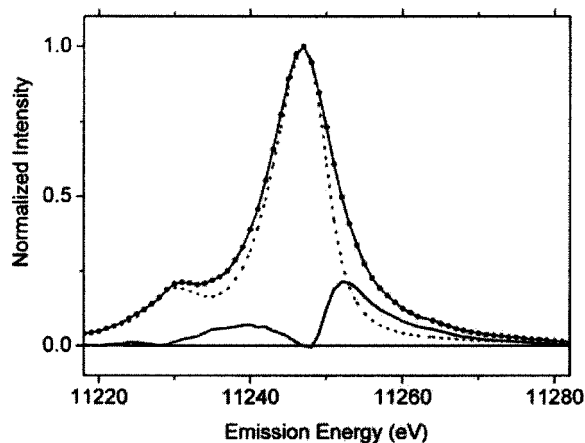

FIG. 2. The $2p_{3/2}4d$ x-ray emission spectra excited at two different excitation energies, respectively 11 568 eV (dotted) and 11 610 eV (connected points). The solid line indicates the difference spectrum.
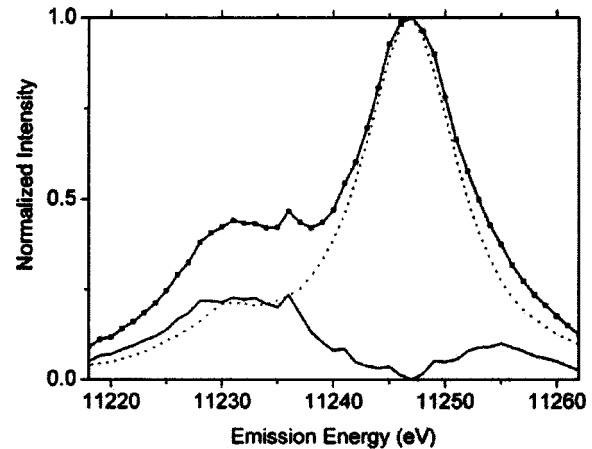

FIG. 3. The $2p_{3/2}4d$ and $2s3p$ x-ray emission spectra excited at respectively 11 610 eV (dotted) and 14 010 eV (connected points). The difference spectrum indicated by the solid line.

eV. In addition the difference spectrum is given: 11 568 eV is exactly at the $2p_{3/2}$ edge position and 11 610 eV can be considered to be a continuum position at 42 eV above the edge. Both spectra show essentially two peaks with an intensity ratio of 9:1. This ratio is determined by the atomic transition cross sections of $4d_{5/2}$ and $4d_{3/2}$ to the $2p_{3/2}$ state. The 11 568 eV edge spectrum is sharper then the 11 610 eV continuum spectrum. This is a consequence of the fact that a maximum in the x-ray absorption spectrum, i.e., in the density-of-states $\rho(\omega)$, will make the x-ray emission spectrum sharper as discussed in Sec. III A.[18] In addition, it can be seen that the sharpening is stronger at the high-energy side, due to the resonant Raman effect at the edge.[19] These modifications in the x-ray emission channel can in turn induce modifications in the x-ray absorption spectrum detected with this emission channel, i.e., at the edge the x-ray emission channel detected x-ray absorption spectrum can deviate from the transmission x-ray absorption spectrum. This effect is related to the possibility to obtain sharp spectra and is a direct consequence of Eq. (1).

Figure 3 shows the x-ray emission spectra at excitation energies of respectively 11 610 eV and 14 010 eV. The x-ray emission spectrum at the excitation energy of 14 010 eV is an addition of the $2p_{3/2}4d$ emission and the $2s3p$ emission channels that accidentally overlap as can be deduced from Table II. The difference between the emission at 14 010 (connected points) and 11 610 (dotted) is the $2s3p$ x-ray emission spectrum, which is indicated by a solid line. The small difference in the respective broadenings on the high-energy side is caused by the different excitation energy. The accidental overlap of the $2p_{3/2}4d$ emission and the $2s3p$ emission channels presents no problem at all for the selective x-ray absorption experiment, because the $2p_{3/2}4d$ emission intensity is essentially constant while scanning over the $2s$ edge. Therefore one can use the $2s3p$ x-ray emission maximum at 11 225 eV for selective $2s$ x-ray absorption.

The experimental broadening of the $2s3p$, $2p_{1/2}3d_{3/2}$, $2p_{3/2}4d_{3/2}$, and $2p_{3/2}4d_{5/2}$ x-ray emission spectra has been derived by fitting a Lorentzian function. The values found have been included in Table II. Neglecting the experimental
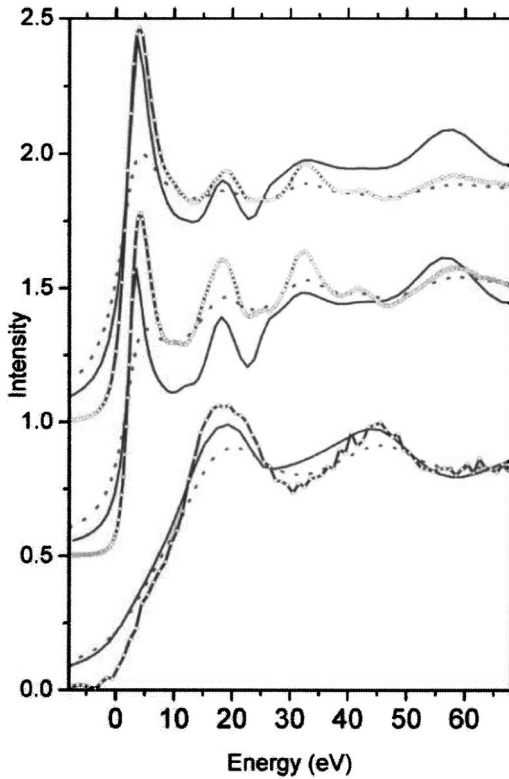
FIG. 4. Top: The L_3 x-ray absorption spectrum (dashed) and the sub-lifetime resolved spectrum detected at the maximum of the $2p_{3/2}4d$ x-ray emission spectrum (solid with open circles) compared with the FEFF8 calculated x-ray absorption spectrum for a Pt$_{55}$ cluster (thin solid line). The same spectra are given for the L_2 edge in the middle and the L_1 edge at the bottom.

broadening of the spectrometer, i.e., a Gaussian function with a resolution of about 0.8 eV, these experimental broadenings should be an addition of the individual broadenings of the core levels in the initial and final states of the x-ray emission process. Assuming that the core hole lifetime broadenings of the $2s$ and $2p$ levels are correct, we find a value of 4.7 for the $4d_{5/2}$ state, which is larger than the photoemission value of 3.6 eV. The $3d_{3/2}$ broadening derived from $2p_{1/2}3d_{3/2}$ x-ray emission is 2.0 eV compared to a value of approximately 3.0 eV from photoemission. The $2s3p$ broadening can not be determined very accurately, but the value of 18 ± 2 eV agrees with the individual $2s$ and $3p$ values.

B. High-resolution XAS spectra

In this section we discuss the use of the x-ray emission channels to measure the x-ray absorption spectra with sub-lifetime resolved resolution, according to Eq. (3). Figure 4 (top) shows the $2p_{3/2}$ x-ray absorption spectrum compared to the sub-lifetime resolved spectrum detected with $2p_{3/2}4d$ x-ray emission. In addition the theoretical density of states has been included, which will be discussed in Sec. IV C. One observes a significant sharpening of the near edge structures. A small part of the sharpening is due to saturation effects in the normal x-ray absorption spectrum, but as this spectrum

has been measured simultaneously we prefer to use it instead of a nonsaturated Pt spectrum. The saturation effects will not affect the discussion of the present paper. A large leading edge is visible in the sub-lifetime spectrum. This structure is related to the empty Pt $5d$ states and its increase in height is largest because it is a sharp structure. All other peaks increase less due to their intrinsic width. The tabulated $2p_{3/2}$ lifetime broadening is 5.3 eV (Ref. 20) (cf. Table II) and using a value of 3.6 for the $4d$ lifetime broadening a value Γ_{SEL} of 3.0 eV is found. We can compare these tabulated values with the experimental Γ_{2p} and Γ_{SEL} from Fig. 4. The experimental values can be found from a Lorentzian fit to the leading edge of the $2p_{3/2}$ spectrum. The experimental broadening effects will be neglected as they can be approximately simulated with a Gaussian of 2.3 eV. In addition the density-of-states does not correspond to a sharp single peak, but to a structure with finite width. We estimate that we can correct for both experimental broadening and the density-of-states effect by subtracting 2.5 eV from the Lorentzian parameters. The experimental values found are respectively 9.2 eV for the normal x-ray absorption spectrum and 4.3 eV for Γ_{SEL}. The corrected values are respectively 6.7 and 1.8 eV. We can rewrite Eq. (2) to

$$\Gamma_{4d}=1/\sqrt{(1/\Gamma_{\mathrm{SEL}}^2)-(1/\Gamma_{2p}^2)}. \tag{4}$$

This yields a $4d$ lifetime broadening of 1.9 eV. The combination of selective x-ray absorption with normal x-ray absorption is thus a good way to determine the life time broadenings of both the initial ($2p$) and final ($4d$) core hole state. The result can be double-checked with the $2p4d$ x-ray emission spectrum. Note that in the case of x-ray emission only the spectrometer resolution is part of the broadening factors, while both the density-of-states effect and the monochromator resolution are not affecting the broadening. From Table II, we find reasonable agreement between these numbers and the tabulated values from XPS.[20]

The middle panel of Fig. 4 shows the $2p_{1/2}$ x-ray absorption spectrum and the sub-lifetime resolved spectrum detected at the $2p_{1/2}3d_{3/2}$ x-ray emission spectrum. The first maximum in the x-ray absorption spectrum turns into a real peak in the selective x-ray absorption spectrum. This shows that there still is a white line related to empty $5d$ states for the $2p_{1/2}$ spectrum, suggesting that the $5d_{3/2}$ valence band is not completely filled. In other words, as discussed above, the $5d_{5/2}$ and $5d_{3/2}$ states are mixed due to crystal field effects according to the numbers given in Table I. The experimental values for the Lorentzian parameter of the broadening are found to be respectively 8.0 eV for the normal x-ray absorption spectrum and 3.1 eV for Γ_{SEL}. These broadenings are less as for the corresponding $2p_{3/2}$ spectra discussed above. The reason is that the density-of-states effect on the broadening is less for the $2p_{1/2}$ spectrum. The $5d$ states can be assumed to be a single peak and only the experimental broadening remains, which we estimate with a subtraction of 1.5 eV. The corrected values are respectively 6.5 eV for the $2p_{1/2}$ lifetime broadening and 1.7 eV for the $3d_{3/2}$ lifetime broadening as derived from Eq. (4). This gives a total broadening $\Gamma_{2p}+\Gamma_{3d}$ of 8.2 eV for the $2p_{1/2}3d_{3/2}$ x-ray emission
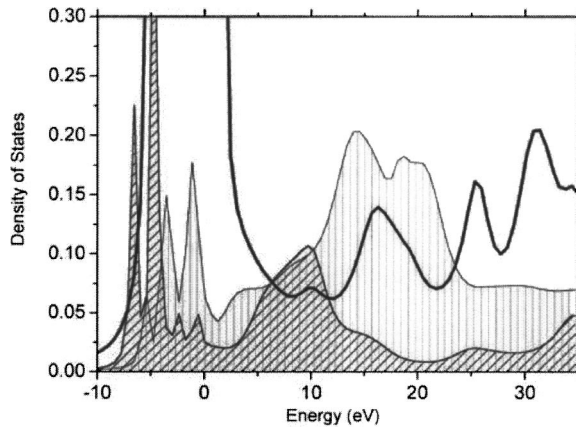
FIG. 5. The density of states of Pt calculated for a Pt_{55} cluster using FEFF8. The s-projected states are diagonally hatched, the p-projected states are vertically hatched, and a solid line represents the d-projected states. The Fermi level indicates the zero of energy.

spectrum, which agrees with the value of 7.9 eV derived from a Lorentzian fit to the x-ray emission spectrum itself.

The bottom of Fig. 4 shows the $2s$ x-ray absorption spectrum compared with the sub-lifetime resolved spectrum detected at the $2s3p$ x-ray emission spectrum. One observes a slow rising edge that reaches a maximum at 13 900. Due to the absence of sharp features, it is not possible to determine reliable experimental broadening factors. The tabulated values for the $2s$ and $3p$ lifetime broadening are respectively 9.4 and 9.0 eV. This yields a value of 6.5 eV for the selective x-ray absorption process and indeed the selective x-ray absorption spectrum is significantly sharper then the normal x-ray absorption spectrum. Fitting the first peak yields a Lorentzian width of respectively 17.5 eV for selective x-ray absorption and 22.5 eV for normal x-ray absorption. This is not an accurate procedure as by far the largest contribution to the broadening is the density-of-states effect. But because the density of states effect is identical in both experiments, this is an experimental proof of the correctness of the use of Eq. 2. If one would replace the lifetime broadening of the $2s$ core hole by the lifetime broadening of the $3p$ core hole nothing would change, as both broadening values are equal.

C. Comparison with calculations

We have performed multiple scattering calculations to determine the Pt $2s$, $2p_{1/2}$, and $2p_{3/2}$ density of states and the corresponding x-ray absorption spectra. Figure 5 shows the density of states around the Fermi level that is set to 0.0 eV. The s, p, and d projected density of states are given. The $5d$ valence band is located between -8 and $+2$ eV. The empty d-states have peaks at 16.1, 25.5, and 31.0 eV. The empty p-states have a double-peaked structure between 13 and 21 eV and the empty s-states have a peak at 10 eV. The Pt $2s$ x-ray absorption spectrum relates to the empty p-states. Both the Pt $2p_{1/2}$ and $2p_{3/2}$ x-ray absorption spectra relate essentially to the empty d-states with a small contribution from empty s-states. At the edge there is a difference between the $2p_{1/2}$ and $2p_{3/2}$ spectrum due to the spin-orbit coupling of
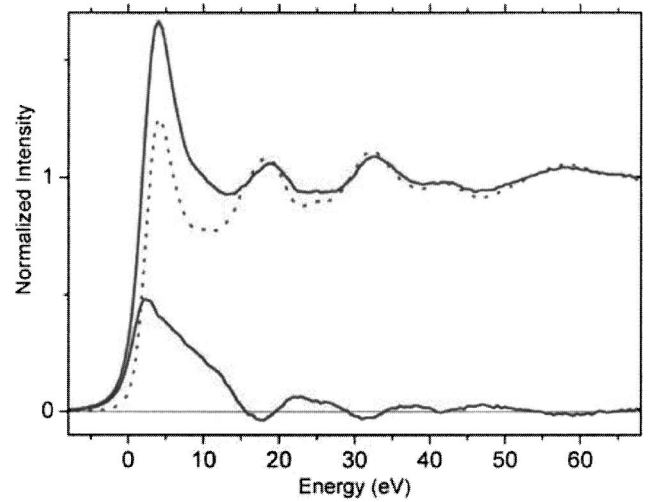

FIG. 6. The difference spectrum (solid) between the $2p_{1/2}$ (dashed) and $2p_{3/2}$ (solid) selective x-ray absorption spectra. The difference between the $5d_{3/2}$ and $5d_{5/2}$ densities of states is equal to 0.87 times this difference.

the $5d$ states and the different matrix elements coupling $2p_{1/2}$ and $2p_{3/2}$ states to respectively the $3d_{3/2}$ and $3d_{5/2}$ states as discussed above.

The calculated spectra are compared with, from top to bottom, the L_3, L_2, and L_1 x-ray absorption spectra in Fig. 4. The lifetime broadening of the theoretical spectrum has been adapted to the selective x-ray absorption spectrum. At the L_3 edge (Fig. 4, top), peaks are visible at 3.8, 17.9, and 32.3 eV corresponding to the peaks in the empty d-states. There is a close correspondence between the selective x-ray absorption spectrum and the theoretical curve; in particular the leading edge and the peak at 17.9 eV are exactly reproduced both in energy and intensity. This confirms that the multiple scattering calculations for the Pt_{55} cluster correctly reproduces the density of states of bulk Pt.

The $2p_{1/2}$ and $2p_{3/2}$ selective x-ray absorption spectra in Fig. 4 are identical apart from the leading edge that is larger in the case of the $2p_{3/2}$ spectrum. Figure 6 shows the difference spectrum between the $2p_{1/2}$ and $2p_{3/2}$ selective x-ray absorption spectra. A nonzero difference is observed only in the region between 0 and 15 eV. This is the region where a difference between the $5d_{3/2}$ and $5d_{5/2}$ densities of states will affect the spectral shape. It follows from Table I and the discussion in Sec. III C that the difference between the $5d_{3/2}$ and $5d_{5/2}$ densities of states is equal to 0.87 times the difference between $2p_{3/2}$ and $2p_{1/2}$ spectrum. The factor of 0.87 can be calculated using the nonzero $2p_{1/2}5d_{5/2}$ intensity and is equal to $(8.6-2*0.4)/9.0$. It is interesting to note that this not only concerns the leading edge, but also the whole energy range up to 15 eV, implying that in this region the $5d_{3/2}$ and $3d_{5/2}$ states are not balanced. Note that the $2p_{1/2}$ spectrum is sharper than the $2p_{3/2}$ spectrum. The reasons are the different final states, respectively $3d$ and $4d$, and a different spectrometer energy resolution.

V. CONCLUDING REMARKS

We have shown for the case of platinum metal that the Pt $2p$ selective x-ray absorption spectrum corresponds to a

sharpened normal x-ray absorption spectrum. The lifetime broadening of the $2p$ core hole is replaced by $\Gamma_{\text{SEL}} = 1/\sqrt{(\Gamma_x^2 + \Gamma_f^2)}$. In the case of a large and a small lifetime broadening, Γ_{SEL} is approximately equal to the small lifetime broadening, i.e., with $\Gamma_x = 10$ and $\Gamma_f = 1$, $\Gamma_{\text{SEL}} = 0.995 \approx 1$. The selective x-ray absorption spectrum therefore provides the density of empty states with a resolution that is essentially determined by the final state. At the moment the overall experimental resolution of approximately 2.3 eV is the limiting factor. A much higher energy resolution can be obtained, as has been shown in an IXS study of Fe_2O_3 in Ref. 21, where an overall experimental resolution of 0.3 eV was obtained. In the case of the Pt *L*-edge an improved monochromator resolution would allow us to further improve the spectral resolution of the obtained density of states to the limits set by the final state lifetime broadening, in the present case around 1.5 eV. The big advantage of a high-resolution hard x-ray determination of the density of states are the possibilities to apply this technique to, for example, high-pressure conditions or to the *in situ* determination of catalysts or batteries during reaction. Many exciting applications could be envisaged.

It is interesting to compare the decrease in lifetime broadening in selective x-ray absorption with the increase in the lifetime broadening of x-ray emission ($\Gamma_{\text{XES}} = \Gamma_x + \Gamma_f$). A combination of x-ray absorption (Γ_x) and selective x-ray absorption (Γ_{SEL}) is able to determine the lifetime broadenings of both the intermediate and final state. These numbers can be cross-checked with the x-ray emission experiment. In the case of both the $2p_{1/2}3d_{3/2}$ and $2p_{3/2}4d_{5/2}$ transitions consistent numbers were found, where it is noted that the determination is complicated by the various experimental and density of states broadening effects that are different for each spectrum. The lifetime broadenings found for the $2p_{1/2}$ and $2p_{3/2}$ core holes were slightly larger than the tabulated values, whereas the values for the $3d_{3/2}$ and $4d_{5/2}$ core holes where a bit smaller. The accuracy in these numbers can be further improved by using a higher experimental resolution. In principle there is no big problem in using an overall experimental resolution of 0.3 eV. This will allow for the detailed determination of the $2p$, $3d$, and $4d$ core hole lifetime broadenings. It would be very interesting to determine the lifetime broadenings for a series of elements and to compare them with the tabulated values from photoemission.

It was shown that the rule of a 6:1:0:5 ratio for respectively the $2p_{3/2}5d_{5/2}$, $2p_{3/2}5d_{3/2}$, $2p_{1/2}5d_{5/2}$, and $2p_{1/2}5d_{3/2}$ transitions are not exactly correct. The atomic ratio is 9:1:0:5, but if one includes crystal field and/or band structure effects, the $2p_{1/2}5d_{5/2}$ transition obtains a finite intensity, the reason being that the $5d_{5/2}$-label changes its character from a pure $5d_{5/2}$ state to a nonpure state labeled $5d_{5/2}$. Because the $2p$ and $3d$ branching rules must always be equal to respectively 2:1 and 3:2, the correct ratio for Pt metal is found to be 8.6:1.4:0.4:4.6. This is important if one assigns the difference between the $2p_{1/2}$ and $2p_{3/2}$ spectra to the difference between $5d_{3/2}$ and $5d_{5/2}$ states.

[1] J. J. Rehr and R. C. Albers, Rev. Mod. Phys. **72**, 621 (2000).

[2] F. M. F. de Groot, J. Electron Spectrosc. Relat. Phenom. **67**, 529 (1994).

[3] F. M. F. de Groot, J. C. Fuggle, B. T. Thole, and G. A. Sawatzky, Phys. Rev. B **41**, 928 (1990).

[4] F. M. F. de Groot, J. C. Fuggle, B. T. Thole, and G. A. Sawatzky, Phys. Rev. B **42**, 5459 (1990).

[5] K. Hämäläinen, D. P. Siddons, J. B. Hastings, and L. E. Berman, Phys. Rev. Lett. **67**, 2850 (1991).

[6] I. Coulthard, T. K. Sham, Y. F. Hu, S. J. Naftel, P. S. Kim, and J. W. Freeland, Phys. Rev. B **64**, 115101 (2001).

[7] T. M. Grehk, W. Drube, G. Materlik, J. E. Hansen, and T. K. Sham, J. Electron Spectrosc. Relat. Phenom. **88**, 241 (1998).

[8] T. K. Sham, T. Ohta, J. Yokoyama, Y. Takada, Y. Kitajima, M. Funabashi, and H. Kuroda, J. Electron Spectrosc. Relat. Phenom. **53**, 177 (1990).

[9] W. Drube, A. Lessmann, and G. Materlik, in *Resonant Anomalous X-ray Scattering*, edited by G. Materlik, C. J Sparks, and K. Fischer (Elsevier, Amsterdam, 1994), p. 473.

[10] W. Drube, R. Treusch, and G. Materlik, Rev. Sci. Instrum. **66**, 1616 (1995).

[11] W. Drube, R. Treusch, T. K. Sham, A. Bzowski, and A. V. Solda-tov, Phys. Rev. B **58**, 6871 (1998).

[12] P. W. Loeffen, R. F. Pettifer, S. Mullender, M. A. Vanveenendaal, J. Rohler, and D. S. Sivia, Phys. Rev. B **54**, 14 877 (1996).

[13] P. Carra, M. Fabrizio, and B. T. Thole, Phys. Rev. Lett. **74**, 3700 (1995).

[14] B. Qi, I. Perez, P. H. Ansari, F. Lu, and M. Croft, Phys. Rev. B **36**, 2972 (1987).

[15] Y. Jeon, B. Y. Qi, F. Lu, and M. Croft, Phys. Rev. B **40**, 1538 (1989).

[16] A. L. Ankudinov, B. Ravel, J. J. Rehr, and S. D. Conradson, Phys. Rev. B **58**, 7565 (1998).

[17] F. M. F. de Groot, Chem. Rev. **101**, 1779 (2001).

[18] F. M. F. de Groot, S. Pizzini, A. Fontaine, K. Hamalainen, C. C. Kao, and J. B. Hastings, Phys. Rev. B **51**, 1045 (1995).

[19] K. Hamalainen, S. Manninen, P. Suortti, S. P. Collins, M. J. Cooper, and D. Laundy, J. Phys.: Condens. Matter **1**, 5955 (1989).

[20] J. C. Fuggle and J. E. Inglesfield, *Unoccupied Electronic States* (Springer Verlag, Berlin, 1992).

[21] W. A. Caliebe, C.-C. Kao, J. B. Hastings, M. Taguchi, A. Kotani, T. Uozumi, and F. M. F. de Groot, Phys. Rev. B **58**, 13 452 (1998).